"Reptational" Movements of Single Synthetic Polymer Chains on Substrate Observed by in-Situ Atomic Force Microscopy

Jiro Kumaki,*,† Takehiro Kawauchi,† and Eiji Yashima†,‡

Yashima Super-structured Helix Project, Exploratory Research for Advanced Technology (ERATO), Japan Science and Technology Agency (JST), 101 Creation Core Nagoya, Shimoshidami, Moriyama-ku, Nagoya 463-0003, Japan, and Department of Molecular Design and Engineering, Graduate School of Engineering, Nagoya University, Chikusa-ku, Nagoya 464-8603, Japan

Received September 5, 2005; Revised Manuscript Received November 17, 2005

ABSTRACT: Vital "reptational" movements of isolated synthetic polymer chains on a substrate were imaged by atomic force microscopy (AFM) in the tapping mode. The isotactic poly(methyl methacrylate) molecules deposited on mica have long flexible chains that reptated on the substrate like snakes (caterpillar-like) along their chain directions in humid air. The thin water layer adsorbed on the substrate accelerated these movements. Possible tip scan effects on the observed movements were evaluated and found to be small mainly based on the following points: (1) the directions and time scales of the movements were not related to those of the scan, (2) the movements of the chains during interruption of the scan were similar to the movements during scanning, and (3) the movements were also observed in the frequency modulation mode (namely, "noncontact" mode) in which the tip force acting on the chains is significantly smaller than that in the tapping mode. The dynamic information about single polymer chains will stimulate new insights into the understanding of polymers, especially in surface phenomena, such as adhesion, wetting, and friction, and is also essential for fabricating advanced nanomaterials based on polymers.

1. Introduction

Studies of the dynamics of polymers on substrates are important in order to understand the practically important surface phenomena of polymers, such as adhesion, wetting, friction, etc.[1] The purest approach to this problem should be the direct observation of the dynamics of isolated polymer chains on substrates. In recent years, the direct imaging of isolated polymer chains has been attracting great interest in polymer science. Previous attempts were mainly focused on the visualization of large biomolecules such as DNA by optical microscopy using a fluorescent labeling technique, which allows one to investigate the three-dimensional dynamics of the biomolecules, for example, diffusion in dilute[2,3] or concentrated solutions[4,5] and elongation in flow[6,7] as well as two-dimensional diffusion at the liquid−solid interface[8] and two-dimensional arrays.[9] However, for practically important synthetic polymers, the direct observation of their dynamics is still challenging and remains a very difficult problem because of the smaller size and high mobility of polymers, although their static structures of the single chains can be observed using scanning probe microscopy such as atomic force microscopy (AFM) and scanning tunneling microscopy.[10−17]

In a previous study,[13] we reported that atactic (at-) poly(methyl methacrylate) blocks of a PS-*block*-PMMA block copolymer (PS = polystyrene) deposited on mica from a water surface changed conformations from their originally compressed form into highly elongated ones by exposing the deposited film under humid air (79% relative humidity (RH)) for 1 day, and as a result, the single synthetic polymer chains could be visualized as random coils by AFM for the first time.[13] The adsorbed water layer of ca. 0.5 nm thick on the mica[18] under the humid air accelerated the chain movement. Under the lower humidity condition of ordinary laboratory air at 54% RH, the chain elongations were slower but still clearly recognizable.[13b] It was surprising for us to find that the high-molecular-weight polymer chains (number-average molecular weight (M_n) of the PMMA block = 3.92×10^5) move on the substrate. The chains should move on the substrate with the monomer units repeatedly attaching and detaching to the substrate. In-situ observation of the chain movements on the substrate should provide molecular level information about the adhesion. This process was, however, too slow to observe their movements in situ by AFM, but this result stimulated us to observe single chain dynamics by reducing their movement by confining them in a thin fluid layer on a substrate.

Since visualization of the PMMA chains, AFM observations of single synthetic polymer chains have been extensively studied, for example, a series of investigations on specially architectured polymers such as polymer brushes[12,14] and monodendron-jacketed polymers[12,15] by Sheiko and Möller, analysis of polyelectrolyte conformations in solutions of various pHs and ionic strengths after frozen on substrates,[16a,b] and observation of a heteroarm star copolymer[16c,d] by Minko and Kiriy, etc.[17]

Recently, Gallyamov, Sheiko, Möller, and co-workers reported the in-situ AFM observations of the reversible conformational transitions of poly(methacrylate)-*graft*-poly(*n*-butyl acrylate) (PMA-*g*-PnBA) brush molecules on mica between aggregated conformations under ethanol vapor and elongated ones under humid air.[19a−c] Similar reversible conformation transitions were also observed for poly(2-vinylpyridine).[19d] These reports clearly indicate that the dynamics of polymer conformational changes under controlled environments could be followed by the tapping mode AFM. Sheiko and co-workers also observed spreading of a melt droplet of a polymer brush (PMA-*g*-PnBA) on highly oriented pyrolytic graphite (HOPG) by in-situ tapping AFM.[20] The brush molecule is a rigid cylindrical polymer with large diameters due to the densely grafted side polymer chains, and easily visualized by AFM; thus,

* Corresponding author. E-mail: kumaki@yp-jst.jp.
† ERATO, JST.
‡ Nagoya University.

10.1021/ma051933o CCC: $33.50
Published on Web 01/07/2006

they could observe the movements of individual brush chains in the spreading droplet as well as the spreading of the droplet itself. However, the movements of the rigid brush polymer chains are different from the ordinal flexible polymer chains as shown here.[13,20]

In this report, we show detailed in-situ AFM observations of the dynamic movements of a flexible synthetic polymer chain on a substrate. Vital movements of the chains along their length were clearly observed in humid air. Detailed movements in air at various humidities as well as possible tip effects on the observed movements will be discussed.

2. Experimental Section

The sample used was an isotactic (it-) PMMA with an M_n of 175 700, a polydispersity index of 1.21, and a *mm* content of 98%, purchased from Polymer Source, Inc. (Montreal, Canada). The polymer was spread from a solution with a polymer concentration of 9.2×10^{-5} g/mL in chloroform (Infinity Pure, Wako Chemicals, Osaka, Japan) onto a water surface (purified by a Milli-Q system) at 25 °C in a commercial Langmuir−Blodgett (LB) trough (FSD-300AS, USI, Japan) and deposited onto a freshly cleaved mica by pulling it out of water (the vertical dipping method). it-PMMA forms an expanded-type surface pressure−area isotherm; thus, the chains are expected to be dispersed on the water surface as isolated chains before compression into a continuous film. Actually, we have successfully deposited polymer chains onto a mica with each chain isolated from the others.[21] The typical deposition conditions included a surface pressure of zero and area of 0.8−2 nm^2/monomer unit; the area is larger than the onset of the surface pressure−area isotherm (0.6 nm^2/monomer unit). AFM observations in a controlled humidity were done using a commercial AFM (NanoScopeIV/multimode AFM unit, Veeco Instruments, Santa Barbara, CA) with the multimode unit being enclosed in a desiccator, where the humidity is controlled by a salt-saturated water solution; NH_4Cl + KNO_3 saturated solution was used for 71% RH. A lower RH was obtained by introducing dry argon. The AFM observations were done with a silicon cantilever (resonance frequency: around 300 kHz; spring constant: ca. 30 N/m) in the tapping mode. The fast scan direction is lateral where the tip always scans both the trace (left to right) and retrace (right to left) irrespective of the scan direction for capturing images, and the slow scan direction is vertical where the tip alternately scans upward then downward. The setting of the free amplitude of the cantilever was typically 2.9 V; this was close to the minimum to obtain clear images of the PMMA chains. To reduce the tapping force, the set point of the amplitude during imaging was maximized within the stable imaging, typically 2.7 V. The tapping force during the measurement typically corresponded to 0.4 nN. AFM images (Figures 1a and 3a and movies S1 (left), S2 (left), and S3−5) are shown in the height mode without any image processing except flattening. AFM images (Figures 1b and 3b, movies S1 (right) and S2 (right)) are shown in the 3D mode with NanoScope software without image processing except flattening; the images are colored with a look-up table having the chains in green and the substrate in red. The movies were constructed from the sequential AFM images canceling the drifts of the images manually. The image analysis was done by ImageJ, a public domain software from the National Institute of Health using the moment calculator plug-in by F. Richard.

3. Results and Discussion

3.1. Selection of Experimental System. As mentioned in the Introduction, the elongation of at-PMMA chains on the mica took about 1 day in the humid air; therefore, this movement is too slow to be observed by in-situ AFM observation. Actually, preliminary experiments showed no detectable conformational changes. The properties of the PMMAs strongly depend on their stereoregularities. The glass transition temperature (T_g) of it-PMMA is around 40 °C, significantly lower than those of the syndiotactic (st-) and at-PMMAs (around 105 °C), indicating that the it-PMMA chains are more flexible than the st- and at-PMMAs. Although it is not adequate to discuss the properties of isolated chains using the bulk T_g, it may qualitatively reflect the flexibility of the single chain. The movement of the PMMA chains on the mica was accelerated by a thin water layer adsorbed under highly humid air. In general, bulk water is not a solvent for PMMAs, but in this case, we should consider the interaction between the PMMA chain and the thin water layer. it-PMMA forms expanded monolayers on the water surface; on the other hand, the st- and at-PMMAs form compressed monolayers.[13,21,22] Scaling analysis of the surface pressure−area isotherms indicated that the water surface is a good solvent for it-PMMA, but not for the st- and at-PMMAs.[21] The AFM images of the PMMA monolayer deposited on mica from the water surface in a dilute state (surface pressure = 0 mN/m) showed elongated single chains separately deposited on the mica for the it-PMMA.[21] On the other hand, the st- and at-PMMAs showed aggregated structures.[13,21] This also indicated that the water surface is a good solvent for it-PMMA. On the basis of the highly flexible chain nature and the good solubility in thin water layer, it-PMMA is expected to be more mobile than the st- and at-PMMAs. Also, the fact that it-PMMA forms elongated conformations both on a water surface and on mica is adequate for the observation of the chain movements under various humidities because the it-PMMA chains do not aggregate under high humidity conditions. On the basis of these reasons, we selected it-PMMA for the in-situ AFM observations.

3.2. Chain Movements under High Humidity. Parts a and b (3D image of the part a) of Figure 1 are AFM images of the it-PMMA chains deposited from the water surface onto a mica by the LB technique in an area of 0.8 nm^2/monomer unit which is wider than the onset of the surface pressure−area isotherm (0.6 nm^2/monomer unit). As shown in Figure 1a,b, the it-PMMA chains were deposited on a mica surface as isolated single chains; the average thickness of the chains was ca. 0.3 nm, and each chain is indicated by a to p.

The movements of the it-PMMA chains in Figures 1a (and 1b) were followed by AFM in the tapping mode at 71% RH for 82.5 min at 2.84 min intervals (total of 29 images were taken) and further followed for 54 min (19 images) after reducing the RH to 54% RH. The AFM unit was enclosed in a desiccator, where the humidity was controlled by a salt-saturated water solution. The movie constructed from the series of images clearly shows significant movements of each chain (see movie S1 in the Supporting Information). The trajectories of the center of mass of each chain in the different RHs are shown by the blue (71% RH) and red lines (54% RH) in Figure 1a. The directions of the movements are random, and the movement was significantly suppressed by reducing the humidity (see red lines at 54% RH). The chains indicated by the white characters (a, b, g, h, and j) moved freely without a permanently adsorbed point, while the chains indicated by light blue (c, d, e, f, i, k, l, m, n, o, and p) are anchored on the substrate by at least one point on the chain throughout the observations. The typical movements of some chains are shown in Figure 1c. The freely moving chain g moved along the chain length. The movement of chain j was somewhat complicated; first the chain went down and then went up, but still tracing the original chain conformations. Chain h originally had a relatively compressed conformation and moved irregularly at first, but soon uncoiled again along its chain length. These unique movements of the polymer chains reminded us of the "reptation model", which successfully describes the diffusion of a chain in a melt in which the model

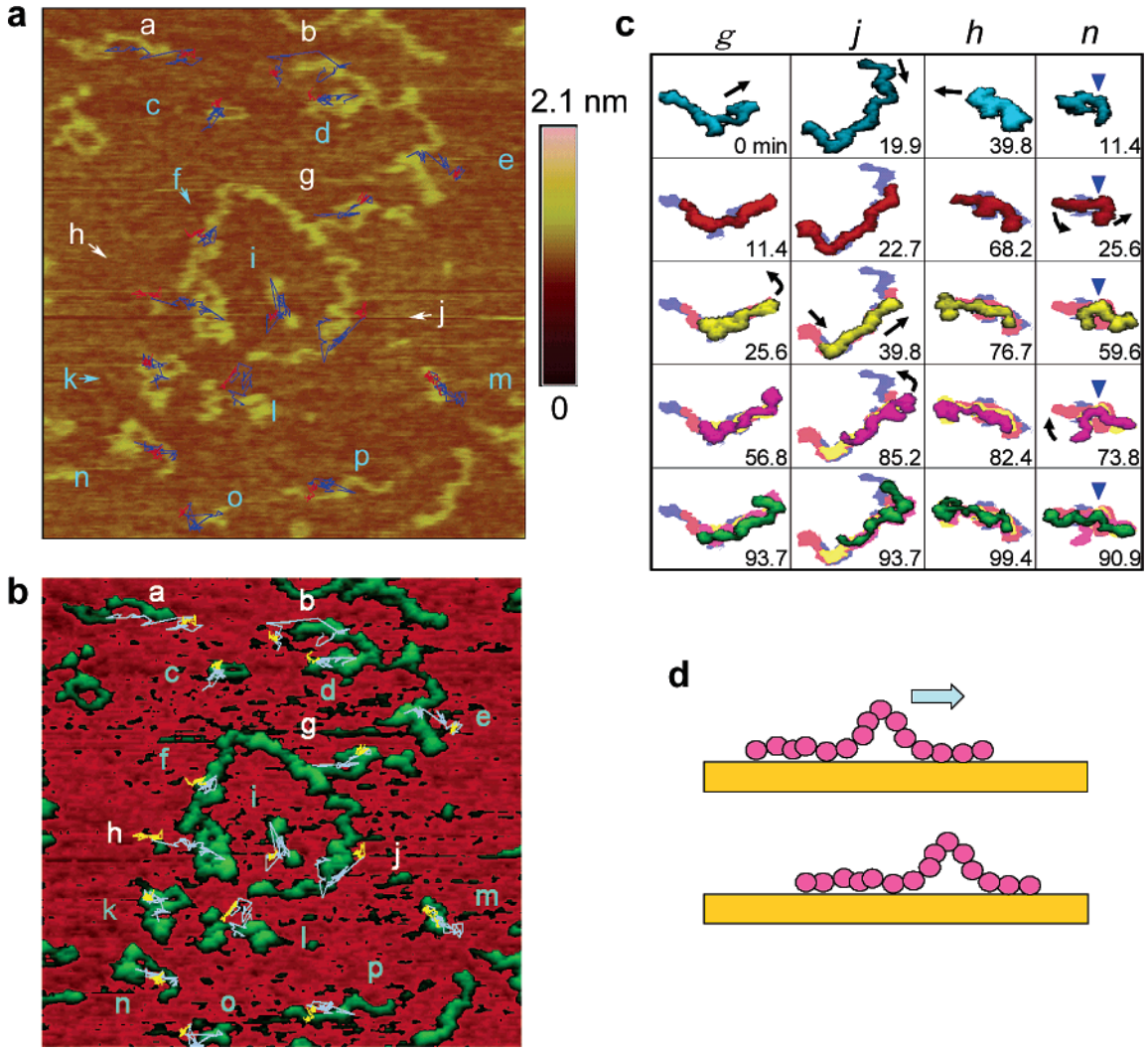

Figure 1. Movements of it-PMMA chains on mica under high humidity. (a) AFM image of it-PMMA chains on mica deposited by LB technique (time: 0 min; scale: 484 × 533 nm; scan direction: left to right). Each chain is indicated by a to p (freely moving chains: white; anchored chains: light blue). The trajectories of the center-of-mass of the chains are shown by blue lines from 0 to 82.5 min in 71% RH and by red lines from 82.5 to 136.5 min in 54% RH. See movie S1 in the Supporting Information. (b) 3D image of Figure 1a. The substrate surface is tilted 25° forward around the lateral axis. The chains and the substrate are shown in green and red, respectively. (c) Time lapse of the chain shapes for chains, g, j, h, and n in Figure 1a (1b). The chain images are superimposed by changing the color from blue, orange, yellow, pink, and green with time. (d) A schematic representation of chain movements on a substrate.

polymer chains move snake-like along their own lengths to avoid strong topological entanglements present in a melt,[23] while in the present dilute system, the physical origin of the constraints that suppress the lateral motion should be very different. Figure 1d shows a schematic representation of a polymer chain moving on a substrate. Each monomer unit reversibly adheres to the substrate. If a loop occurs, it should move along the chain length; as a result, the chain should move along the length. This caterpillar-like motion may explain the chain movements along its length observed here. On the other hand, chains, a part of which are anchored on the substrate throughout the observation, moved very differently. Chain n in Figure 1c swung laterally around the anchored point which is indicated by the blue arrow. These lateral motions are typically observed for fixed chains (for example, see chain e in movie S1). Considering a real caterpillar moving on a board, if we let it freely move, it moves along its length, but if we fix a part of the body, it should move laterally around the fixed part. Although the origins of the movements are quite different (a thermal Brownian motion for a polymer chain vs a motion by the belly muscles for a real caterpillar), the movements of the polymer chains seem to qualitatively resemble those of the much larger real caterpillars.

Another noticeable feature of the movements is that the chains may have some tendency to move in 3-fold symmetrical directions: vertical, 60° clockwise and anticlockwise. This is not very clear for all chains but typically seen, for example, in the movements of chains g and j (Figure 1c). The directions of the movements, and as a result, the conformations, changed at angles close to 60°or 120°. The mica surface has a pseudohexagonal two-dimensional lattice;[24] therefore, the it-PMMA chains may move along the 3-fold symmetrical axes of the lattice. We have experienced that the compressed it-PMMA monolayers deposited on the mica in their amorphous state postcrystallized as the orientations of the crystals formed a 3-fold symmetry, indicating that the it-PMMA chains may epitaxially crystallize on the basal plane of the mica. The strong interaction between the it-PMMA chain and the mica crystal may rationalize the preferential movements of the chains along the crystal lattices.

In this report, we focused on the movements of the freely moving chains. It is not clear at this moment why freely moving chains and anchored chains are mixed and why the anchored points are more strongly adhered to the substrate. We cannot really understand the adhesion phenomena of the polymer chains

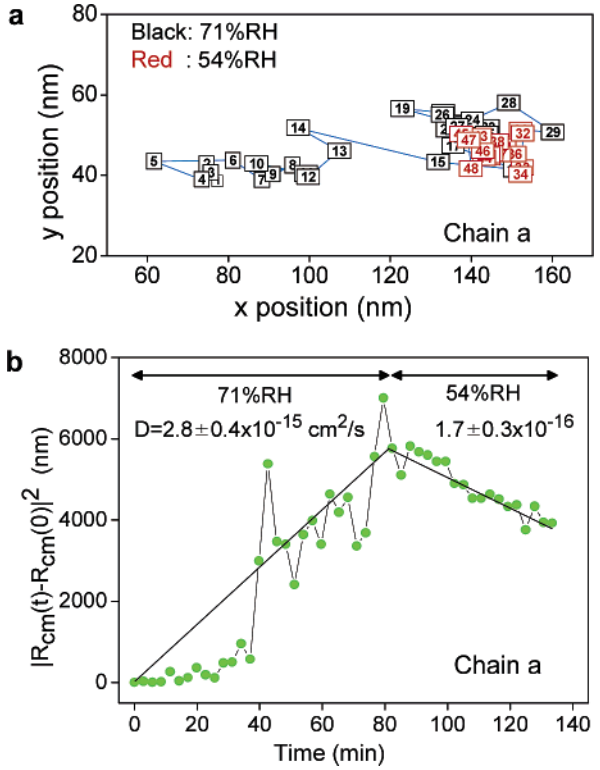

Figure 2. Analysis of the movements of it-PMMA chains. (a) Trajectories of the center-of-mass of chain a in Figure 1a (1b). (b) Time dependence of the square displacement of the center-of-mass of chain a.

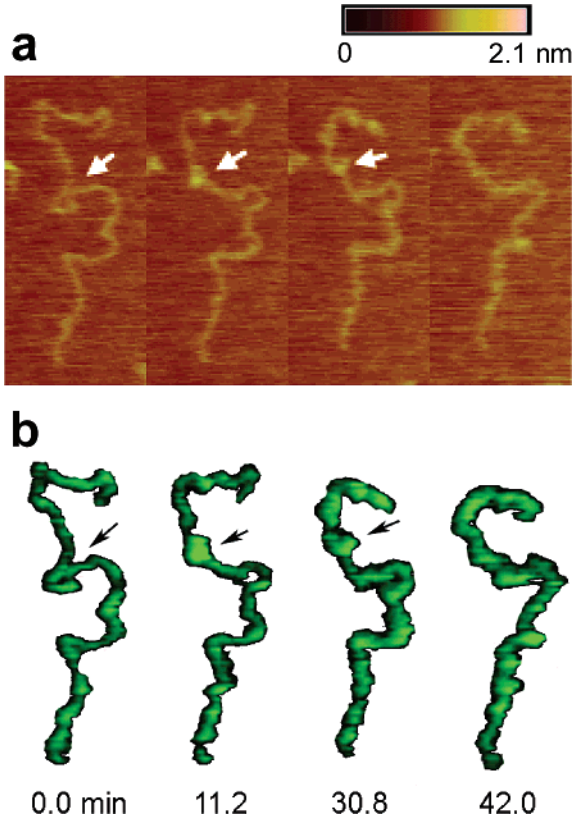

Figure 3. Movements of an it-PMMA chain on mica at lower humidity. (a) Time-lapse AFM images of it-PMMA chains at 34% RH. The arrow indicates movements of a loop along the chain. Scale: 121 × 264 nm; scan direction: right to left. (b) Chain images from 3D AFM image of Figure 3a. See movie S2 in the Supporting Information.

on a molecular level until we can answer these questions; this should be future work.

Figure 2a,b shows the trajectories of the center-of-mass of chain a and the time dependence of the square of the displacement $|\mathbf{R}_{cm}(t) - \mathbf{R}_{cm}(0)|^2$, where $\mathbf{R}_{cm}(t)$ is the center-of-mass vector of the chain at time t. The diffusion coefficient of the chain, as obtained from the relation of $|\mathbf{R}_{cm}(t) - \mathbf{R}_{cm}(0)|^2 = 4Dt$, was $(2.8 \pm 0.4) \times 10^{-15}$ cm^2/s at 71% RH and significantly decreased to $(1.7 \pm 0.3) \times 10^{-16}$ cm^2/s at 54% RH.[25] The movement is quite sensitive to the humidity, in other words, on the thickness of the adsorbed water on the mica which is ca. 0.35 nm at 71% RH and 0.2 nm at 54% RH.[18] How does the diffusion coefficient depend on the molecular weight? We tried to estimate it. The diffusion coefficient decreased with increase of the molecular weight; however, the small number of scattered data currently makes it difficult to derive any concrete scalings. The power-law scaling previously reported for polymer chain diffusions on substrates was $D \approx N^{-1}$ (where N is the degree of polymerization) for huge DNA chains at a lipid membrane/water interface studied using fluorescent microscopy by Rädler[8,26] and $D \approx N^{-3/2}$ for poly(ethylene glycol) (PEG) at a hydrophobic silica/water interface by fluctuation correlation spectroscopy of the fluorescent probe labeled at the polymer end by Granick.[27] Granick attributed the strong difference in the power laws between the two systems to the difference in the substrates; the former is a fluid lipid membrane, thus the substrate is mobile, on the other hand, the latter is a solid surface. He proposed a reptation model (chains move along their length like snakes) to explain their −3/2 scaling, reserving a variety of other possible models which explain the scaling, such as an amoeba model (close-packed chain with relatively mobile monomers at the perimeter) and a hovercraft model (chain slips on thin fluid layer on substrate), etc.;[27b] the assignment of the mechanism required new experimental evidence to distinguish them. Our observation of the movements of chains on the solid surface supports the reptation mechanism.

The atmosphere of our system is different from the DNA and PEG systems (air in our study vs water in the DNA and PEG systems); thus, the constraint of the movements is much stronger in our case. As a result, the diffusion coefficient (10^{-15} cm^2/s) is much smaller than that of the DNA (10^{-9} cm^2/s) and PEG systems (10^{-11} cm^2/s, estimated for the same molecular weight).

3.3. Chain Movements under Low Humidity. Figure 3 shows the movement of the it-PMMA chains at 34% RH; the thickness of the adsorbed water layer was ca. 0.1 nm.[18] At the lower RH, the mobility reduction prohibited lateral diffusion of the chains but enabled one to see detailed conformational changes. A loop indicated by the arrow moved along the chain in a manner similar to that schematically shown in Figure 1d (see movie S2 in the Supporting Information; much smaller movements along the chain are also recognizable at the lower side of the same chain). Movie S3 in the Supporting Information shows the movements of the it-PMMA chains under a much drier condition, 5% RH, in high resolution. The conformational changes looked almost stopped at a low magnification; however, the slow but vital movements of small loops were clearly visible at a high magnification.

3.4. Discussion on Possible Tip Effect on the Chain Movements. In the AFM measurements, a possible tip effect on the chain movements should be considered. It might not be perfectly avoidable in the AFM measurements, but we think the movements observed here mainly reflect the true movement of the chains as discussed below.

First, the movements of the chains, not only the overall movements of the chains but also each displacement between

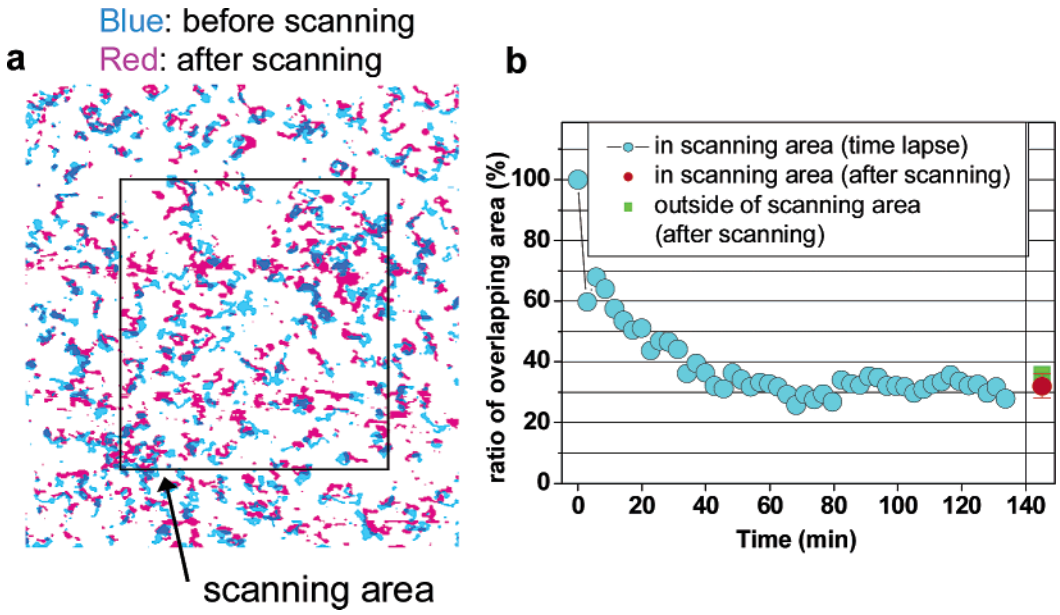

Figure 4. Comparison of chain movements inside and outside the long-term scanning area. (a) Low-magnification AFM images before (blue) and after (red) the long-time-scanning of movie S1 (Figure 1a). Movie S1 (Figure 1a) is a part of the scanning area indicated by the square. Binarized image; scale: $1.75 \times 1.88\ \mu$m. (b) Time dependence of the ratio of overlapping area of chain images between the first image and the later images of movie S1 (Figure 1a) (blue full circles) and the overlapping ratios between before and after the long-term-scan in (a) (red full circle: in the scanning area; green full square: outside the scanning area).

subsequent images, were random and not related to the scan directions (see Figure 1a and movie S1). The total center-of-mass of 16 chains in Figure 1a was within the standard deviation of 7 nm throughout the observations, which also indicates no systematic movement (see movie S3 in the Supporting Information for comparison between chain movements and both the fast (trace and retrace) and slow (upward and downward) scan directions of each image which constitutes the movie).

Second, the time scale of the movements was on the order of several tens of minutes and much longer than that of the scanning time scale (20 s for the fast scan (lateral) and 2.84 min for the slow scan (vertical)) (see movie S3).

Third, chain movements outside the long-term-scan area are compared with those inside the area. Figure 4a shows lower magnification AFM images taken before (shown in blue) and after (shown in red) the long-time scan for Figure 1 (movie S1); Figure 1 (movie S1) corresponds to part of the scanning area indicated by the square. There is no qualitative difference between the inside and outside the scanning area after the long-time scan. Figure 4b shows the time dependence of the ratio of the chain-overlapping area between the first image and the later images of movie S1 (shown in blue full circle). With the movements of the chains, the overlapping ratio gradually decreased from 100% to about 30% and became almost constant after the RH was reduced to 54% at 82.5 min. The overlapping ratios between before and after the long-time scan in Figure 4a are denoted by the red full circle (inside the scan area) and the green full square (outside the scan area). The ratio inside the scan area is in good agreement with that from the movie. The ratio outside the long-time-scan area is 36%, very close to that inside the scan area. On the basis of the fact that the outside area was scanned only two times, if the chains had thoroughly moved due to the tip effect, the ratio should have been 60−70%. We cannot explain these results without assuming spontaneous movements of the chains without any tip effect.

Fourth, the chain movements during an interruption of the tip scan are discussed here.[28] Figure 5 shows the movements of the it-PMMA chains at 71% RH. The scanning was interrupted for 40 min from 150 to 190 min as indicated by the shadowed region. A chain indicated by a blue ellipsoid was firmly anchored to the mica throughout the observation; thus, the square displacement was constant. A chain indicated by a pink ellipsoid was a freely moving chain. The conformations of the pink chain immediately before and after the interruption of the scan were significantly different, and the movement of the center-of-mass during interruption was noticeable and fairly comparative to the movement before and after the interruption of the scan although the data are somewhat scattered. The diffusion coefficient derived from the slope was 3.1×10^{-15} cm^2/s, which reasonably agrees with the data in Figure 2. These results indicate the chains can move without the tip effect, and the tip effect on the movements is small.

Fifth, the chain movements were observed by the frequency-modulation AFM (commonly called "noncontact" AFM). In the tapping mode, the amplitude of the cantilever oscillation during imaging (A_{imaging}) is reduced from the amplitude of the free oscillation of the cantilever (A_{free}), and this reduction in the amplitude of the cantilever oscillation is used for the feedback signal for imaging in the tapping mode AFM. In our case, we minimized the reduction of the amplitude to as low as possible within the stable imaging as $A_{\text{imaging}}/A_{\text{free}} = 0.93$. Although this was a very light tapping condition, the chains were still being tapped by the cantilever during imaging. On the other hand, in the "noncontact" mode, A_{imaging} is equal to A_{free}, and the frequency shift of the cantilever oscillation caused by the cantilever approaching the sample is used as a feedback signal for imaging; therefore, the tip force acting on the sample is significantly smaller than the tapping mode AFM.[29] We observed movements of the it-PMMA chains on mica under 34% RH by "noncontact" AFM. Under this dry condition, lateral diffusions of the chains were prohibited, but vital movements in the chains were clearly seen; see movie S5 in the Supporting Information. This may also indicate that the movements of the it-PMMA chains are not caused by the strong force from the cantilever.

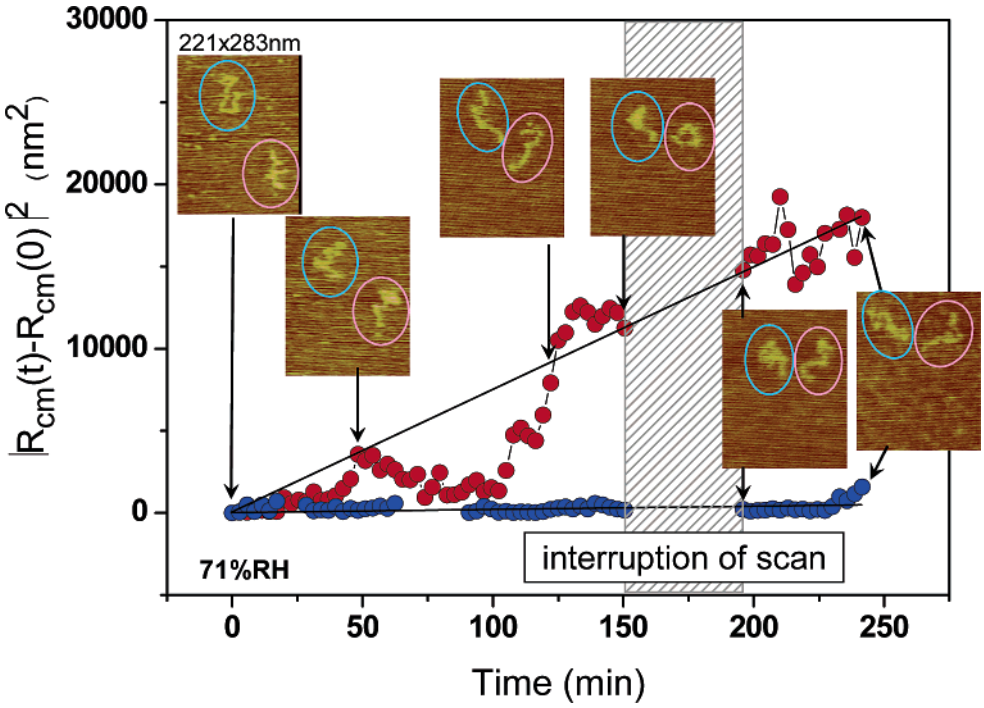

Figure 5. Time dependence of the square displacement of the center-of-mass of two it-PMMA chains along with time-lapse AFM images of the chains at the time indicated by the arrows. Blue and pink data points correspond to the chain images indicated by the same colors. The scanning was interrupted from 150 to 190 min as indicated by the shadow region.

We have shown here that the movements of the it-PMMA chains observed here may not be due to the tip effect and the effect should be small based on the following evidence: (1) the directions and time scales of the movements were not related to those of the scan, (2) the movements of the chains outside the long-term-scanning region were similar to those inside the scan region, (3) the chain movements during interruption of the scan were similar to those during scanning, and (4) the movements were observed by "noncontact-mode" AFM in which the tip force acting on the chains are significantly smaller than that of the tapping mode.

AFM researchers may have some experience in observing forced chain movements due to strong tip effects. The reptational movements of the it-PMMA observed here are very different from them. The strong tip effects usually make all chains move in one direction, either the trace or retrace fast scan direction, and the chain movement shows no specific feature such as reptational movements as shown here but shows forced one-directional movements irrespective of the chain conformations. For example, the movements of the loop-shape chain in the supporting movie S3 moved along its loop; thus, the directions of the movements of each part of the chain are different. This movement is not possible by the strong tip effect. Skeptical readers may suspect if the tip force is not strong enough to produce a systematic motion but is strong enough to cause random motions in each part of the chains; reptational movements here might be observed. We do not deny the possibility that the small tip effects may somewhat accelerate the random motion of the chains. If the tapping force acting on parts of the chain accelerates random movements of the chain parts through a repulsive or attractive interaction with the tip, it may cause similar movements of the chain. In this case, the tip force acts as an accelerator of the thermal Brownian motion of the chain parts, and as a result, the movements should be qualitatively similar to the movements of the chain without any tip effect; in other words, the reptational feature observed here may reflect the true movements of the chain. However, we would like to note that the acceleration effect by the tip might be small in our case based on the results of the scan interruption study (Figure 5) and the evaluation of the chain movements outside the long-term scan region (Figure 4), as mentioned above.

We would like to discuss why a moving polymer chain can be visualized by AFM. Polymer chains should move on the substrate with the monomer units repeatedly attaching and detaching to the substrate. If the molecular weight of the polymer is sufficiently high, at a given time, the chain is attached to the substrate by a sufficient number of repeating units, thus possibly standing against the tip force.

Sheiko mentioned in their report[20] an attempt to observe the thermal diffusion of isolated polymacromer molecules (PMA-*g*-PnBA) on HOPG and concluded that significant tip effects were unavoidable. The polymacromer is a rigid cylindrical polymer with densely grafted side polymer chains, thus the mobility is small, and the interaction between HOPG and the polymer is expected to be very small, thus their system was a rigid polymer with a small mobility on a slippery surface. This may be the reason why the tip effect was not avoidable. On the other hand, our system is a flexible chain with a high mobility. The mobility is even enhanced by the adsorbed water layer, and it is deposited on the surface which strongly interacts with the polymer. Previously, we reported that no detectable conformational changes in the at-PMMA chains on mica was observed by repeated AFM scanning.[13b] This indicates that, without the high mobility of the PMMA chains, the adhesion between the PMMAs and mica is strong. The high mobile polymer and the strongly interacting surface may explain the small tip effect in our system.

4. Concluding Remarks

We have shown experimental evidence that "reptational" movements of synthetic polymer chains on a substrate were observed by AFM. To observe the dynamics of the chains by AFM, the movements should be adjusted within a range where

the movements are in the time scale of the AFM measurement, and the affinity of the chains to the substrate is sufficient to overcome the tip effect. In this report, this was done by selecting the polymer/substrate system and adjusting the thickness of the adsorbed water layer, but this could also be done using other parameters, such as temperature and various organic atmospheres. Dynamic information on a molecular level should improve our understanding of the surface phenomena. Polymer chains on substrates are some of the essential parts when fabricating advanced nanomaterials; thus, this dynamic information should provide a new insight and open possibilities for nanomaterials with dynamic functions.

Supporting Information Available: Movies of Figures 1 and 3 (movies S1 and S2); movie which compares the polymer chain movements with the AFM scan directions of each image (movie S3); movie of the chain movements at 5% RH (movie S4); movie of the chain movements observed by the noncontact AFM (movie S5). This material is available free of charge via the Internet at http://pubs.acs.org.

References and Notes

(1) For a recent review, see: Granick, S.; Kumar, S. K.; Amis, E. J.; Antonietti, M.; Balazs, A. C.; Chakraborty, A. K.; Grest, G. S.; Hawker, C.; Janmey, P.; Kramer, E. J.; Nuzzo, R.; Russell, T. P.; Safinya, C. R. *J. Polym. Sci., Part B: Polym. Phys.* **2003**, *41*, 2755.

(2) Matsumoto, M.; Sakaguchi, T.; Kimura, H.; Doi, M.; Minagawa, K.; Matsuzawa, Y.; Yoshikawa, K. *J. Polym. Sci., Part B: Polym. Phys.* **1992**, *30*, 779.

(3) Smith, D. E.; Perkins, T. T.; Chu, S. *Macromolecules* **1996**, *29*, 1372.

(4) Käs, J.; Strey, H.; Sackmann, E. *Nature (London)* **1994**, *368*, 226.

(5) Perkins, T. T.; Smith, D. E.; Chu, S. *Science* **1994**, *264*, 819.

(6) de Gennes, P.-G. *Science* **1997**, *276*, 1999.

(7) Perkins, T. T.; Smith, D. E.; Chu, S. *Science* **1997**, *297*, 2016.

(8) Maier, B.; Rädler, J. O. *Phys. Rev. Lett.* **1999**, *82*, 1911.

(9) Nykypanchuk, D.; Strey, H. H.; Hoagland, D. A. *Science* **2002**, *297*, 987.

(10) Magonov, N. S. In *Encyclopedia of Analytical Chemistry*; Meyers, R. A., Ed.; John Wiley & Sons: Chichester, 2000; p 7432.

(11) Sheiko, S. S. *Adv. Polym. Sci.* **2000**, *151*, 61.

(12) Sheiko, S. S.; Möller, M. *Chem. Rev.* **2001**, *101*, 4099. In a part of this review, movements of rigid-rod monodendron-jacketed polymer chains sliding on a HOPG are reported. Their sliding movements are quite different from those of the flexible chains reported here.

(13) (a) Kumaki, J.; Nishikawa, Y.; Hashimoto, T. *J. Am. Chem. Soc.* **1996**, *118*, 3321. (b) Full paper version of a communication (a) see: Kumaki, J.; Hashimoto, T. *J. Am. Chem. Soc.* **2003**, *125*, 4907.

(14) (a) Sheiko, S. S.; Gerle, M.; Fischer, K.; Schmidt, M.; Möller, M. *Langmuir* **1997**, *13*, 5368. (b) Gerle, M.; Fischer, K.; Roos, S.; Müller, A. H. E.; Schmidt, M.; Sheiko, S. S.; Prokhorova, S.; Möller, M. *Macromolecules* **1999**, *32*, 2629. (c) Sheiko, S. S.; Prokhorova, S. A.; Beers, K. L.; Matyjaszewski, K.; Potemkin, I. I.; Khokholov. A.; Möller, M. *Macromolecules* **2001**, *34*, 8354. (d) Sheiko, S. S.; da Silva, M.; Shirvaniants, D.; LaRue, I.; Prokhorova, S.; Möller, M.; Beers, K.; Matyjaszewski, K. *J. Am. Chem. Soc.* **2003**, *125*, 6725.

(15) (a) Percec, V.; Ahn, C.-H.; Ungar. G.; Yeardley, D. J. P.; Möller, M.; Sheiko, S. S. *Nature (London)* **1998**, *391*, 161. (b) Prokhorova, S. A.; Sheiko, S. S.; Ahn, C.-H.; Percec. V.; Möller, M. *Macromolecules* **1999**, *32*, 2653. (c) Prokhorova, S. A.; Sheiko, S. S.; Mourran, A.; Azumi, R.; Beginn, U.; Zipp, G.; Ahn, C.-H.; Holerca, N.; Percec, V.; Möller, M. *Langmuir* **2000**, *16*, 6862.

(16) (a) Minko, S.; Kiriy, A.; Gorodyska, G.; Stamm, M. *J. Am. Chem. Soc.* **2002**, *124*, 3218. (b) Kiriy, A.; Gorodyska, G.; Minko, S.; Jaeger, W.; Štěpánek, P.; Stamm, M. *J. Am. Chem. Soc.* **2002**, *124*, 13454. (c) Kiriy, A.; Gorodyska, G.; Minko, S.; Stamm, M.; Tsitsilianis, C. *Macromolecules* **2003**, *36*, 8708. (d) Gofodyska, G.; Kiriy, A.; Minko, S.; Tsitsilianis, C.; Stamm, M. *Nano Lett.* **2003**, *3*, 365.

(17) (a) Barner, J.; Mallwitz, F.; Shu, L.; Schlüter, A. D.; Rabe, J. P. *Angew. Chem., Int. Ed.* **2003**, *42*, 1932. (b) Zhuang, W.; Ecker, C.; Metwelaar, G. A.; Rowan, A. E.; Nolte, R. J. M.; Samorí, P.; Rabe, J. *Macromolecules* **2005**, *38*, 473. (c) Sakurai, S.; Ohira, A.; Suzuki, Y.; Fujito, R.; Nishimura, T.; Kunitake, M.; Yashima, E. *J. Polym. Sci., Part A: Polym. Chem.* **2004**, *42*, 4621.

(18) Beaglehole, D.; Radlinska, E. Z.; Ninham, B. W.; Christenson, H. K. *Phys. Rev. Lett.* **1991**, *66*, 2084.

(19) (a) Gallyamov, M. O.; Tartsch, B.; Khokhlov, A. R.; Sheiko, S. S.; Börner, H. G.; Matyjaszewski, K.; Möller, M. *Chem.—Eur. J.* **2004**, *10*, 4599. (b) Gallyamov, M. O.; Tartsch, B.; Khokhlov, A. R.; Sheiko, S. S.; Börner, H. G.; Matyjaszewski, K.; Möller, M. *Macromol. Rapid Commun.* **2004**, *25*, 1703. (c) For similar conformational transition under different vapors, see: Gallyamov, M. O.; Tartsch, B.; Khokhlov, A. R.; Sheiko, S. S.; Börner, H. G.; Matyjaszewski, K.; Möller, M. *J. Microsc.* **2004**, *215*, 245. (d) Gallyamov, M. O.; Khokhlov, A. R.; Möller, M. *Macromol. Rapid Commun.* **2005**, *26*, 456.

(20) Xu, H.; Shirvanyants, D.; Beers, K.; Matyjaszewski, K.; Rubinstein, M.; Sheiko, S. S. *Phys. Rev. Lett.* **2004**, *93*, 20613-1.

(21) Kumaki, J.; Kawauchi, T.; Yashima, E. *J. Am. Chem. Soc.* **2005**, *127*, 5788.

(22) Brinkhuis, R. H. G.; Schouten, A. J. *Macromolecules* **1991**, *24*, 1487.

(23) Doi, M.; Edwards, S. F. *The Theory of Polymer Dynamics*; Oxford Science Publication: Oxford, 1986.

(24) (a) Kern, R. In C*rystal Growth in Science and Technology*; Arend, H., Hulliger, J., Eds.; Plenum Press: New York, 1989; p 143. (b) Liu, X.; Zhang, Y.; Goswami, D. K.; Okasinski, J. S.; Salaita, K.; Sun, P.; Bedzyk, M. J.; Mirkin, C. A. *Science* **2005**, *307*, 1763.

(25) The positions of dust which existed just next to the area of Figure 1a (movie S1) were within the standard deviation of 2 nm, which corresponds to an error in the diffusion coefficient of less than 7×10^{-17} cm^2/s.

(26) Maier, B.; Rädler, O. *Macromolecules* **2000**, *33*, 7185.

(27) (a) Sukhishvili, S. A.; Chen, Y.; Müller, J. D.; Gratton, E.; Schweizer, K. S.; Granick, S. *Nature (London)* **2000**, *406*, 146. (b) Sukhishvili, S. A.; Chen, Y.; Müller, J. D.; Gratton, E.; Schweizer, K. S.; Granick, S. *Macromolecules* **2002**, *35*, 1776.

(28) We tried to observe the chain movements by increasing the tip force by changing the scan parameters, for example, by decreasing the set point ratio. However, the increase in the tip force made continuous imaging of the polymer chains abruptly disturbed and subsequent imaging impossible; this is probably due to an abrupt attachment of the polymer chain onto the tip. Therefore, instead of this, we tried to evaluate the movements without the tip effect by interrupting the scan during the continuous imaging.

(29) Giessible, F. J. In *Noncontact Atomic Force Microscopy*; Morita, S., Wiesendanger, R., Meyer, E., Eds.; Springer: Berlin, 2002; p 11.

MA051933O